Electronic supplementary information

Fullerene derivative anchored SnO_2 for high-performance perovskite solar cells

Kuan Liu[ab], Shuang Chen[c], Jionghua Wu[b], Huiyin Zhang[b], Minchao Qin[d], Xinhui Lu[d], Yingfeng Tu[c*], Qingbo Meng[b*], and Xiaowei Zhan[a*]

[a] *Department of Materials Science and Engineering, College of Engineering, Key Laboratory of Polymer Chemistry and Physics of Ministry of Education, Peking University, Beijing 100871, China. E-mail: xwzhan@pku.edu.cn*

[b] *CAS Key Laboratory for Renewable Energy, Beijing Key Laboratory for New Energy Materials and Devices, Institute of Physics, Chinese Academy of Sciences, Beijing 100190, China. E-mail: qbmeng@iphy.ac.cn*

[c] *Jiangsu Key Laboratory of Advanced Functional Polymer Design and Application, College of Chemistry, Chemical Engineering and Materials Science, Soochow University, Suzhou 215123, China. E-mail: tuyingfeng@suda.edu.cn*

[d] *Department of Physics, The Chinese University of Hong Kong, New Territories 999077, Hong Kong, China.*

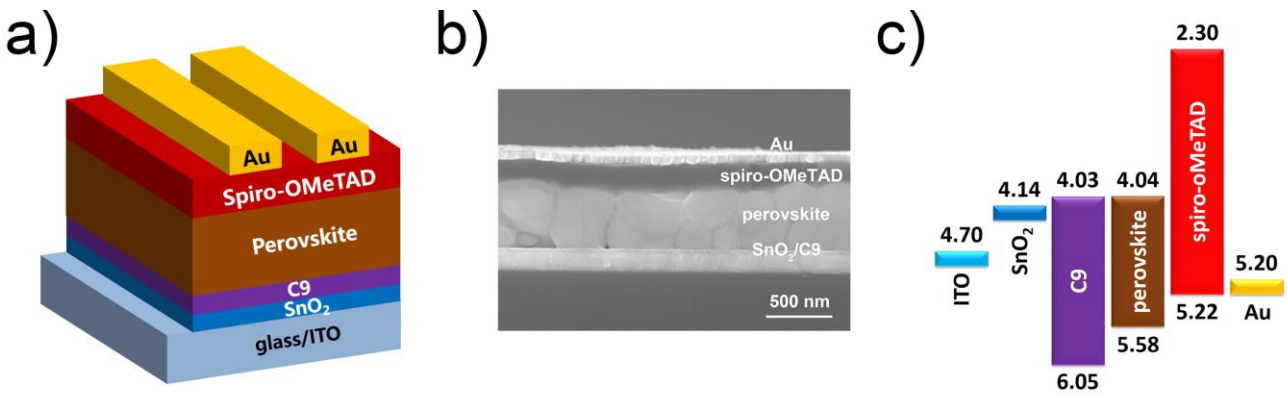

Fig. S1 (a) Schematic device architecture of PHJ PSCs based on C9 modified SnO_2 ETL. (b) Cross-sectional SEM image of a typical C9 modified device. (c) Energy levels diagram of corresponding layers in the device.

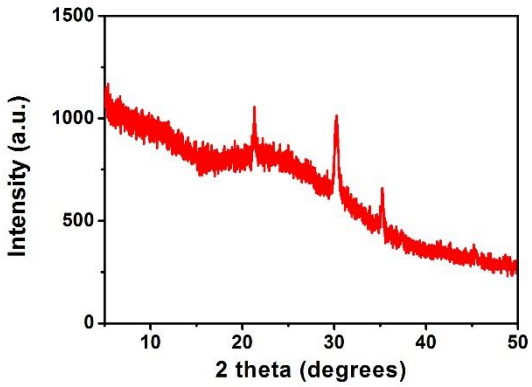

Fig. S2 XRD pattern of the low-temperature processed SnO_2 compact layer.

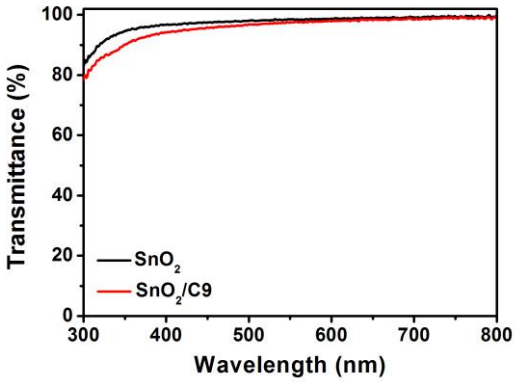

Fig. S3 Transmission spectra of C9 modified and bare SnO_2 deposited on glass substrates.

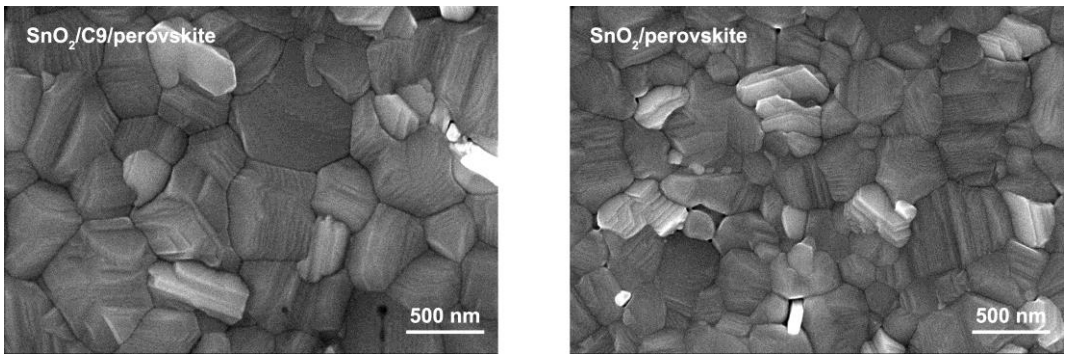

Fig. S4 Top-view SEM images of the perovskite films on C9 modified and bare SnO_2 substrates.

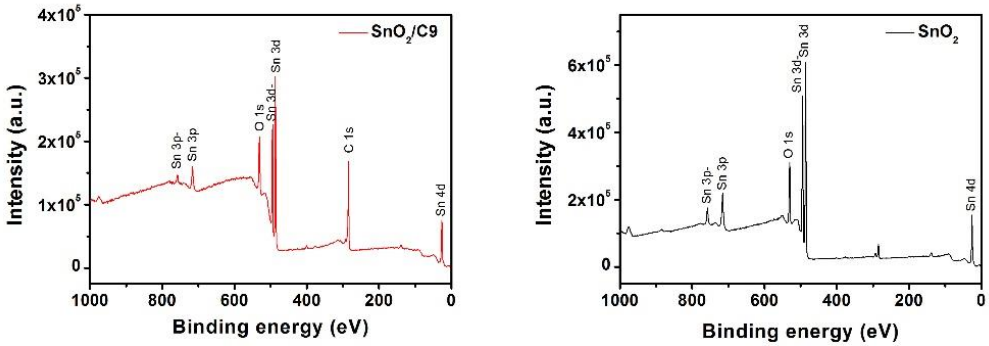

Fig. S5 XPS survey scans for C9 modified SnO_2 and bare SnO_2.

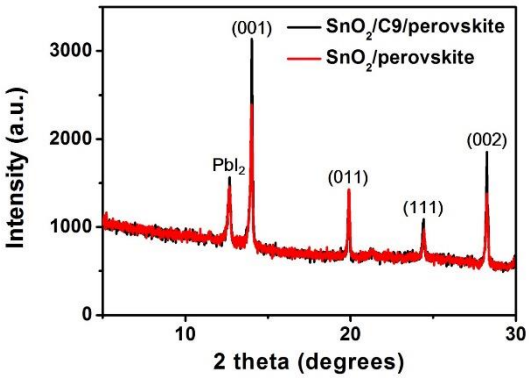

Fig. S6 XRD patterns of the $(FAPbI_3)_x(MAPbBr_3)_{1-x}$ based perovskite on C9 modified and bare SnO_2 substrates.

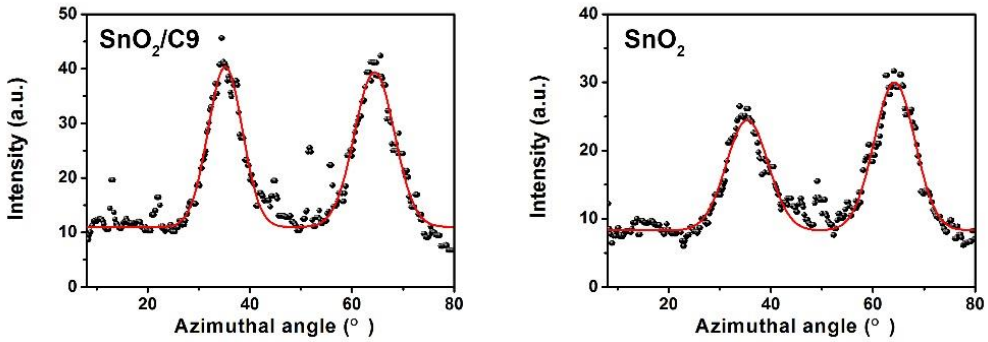

Fig. S7 The polar intensity profiles along the ring in the q_r range of 0.98 to 1.02 $Å^{-1}$ for the perovskite films deposited on C9 modified and bare SnO_2, respectively.

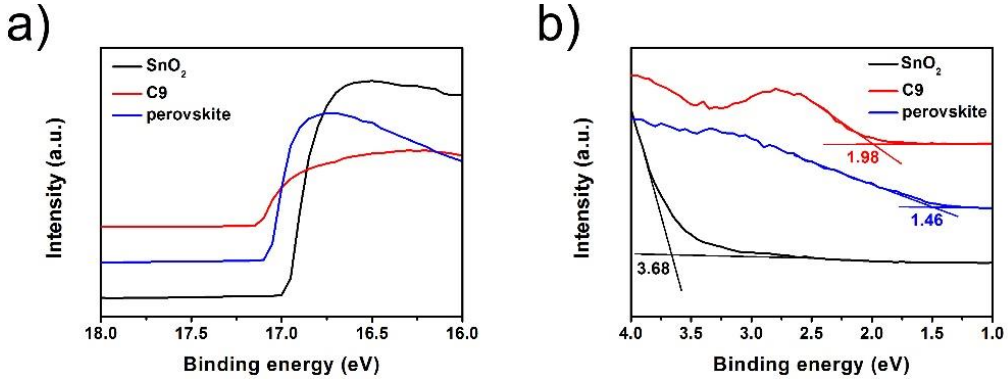

Fig. S8 UPS results of SnO_2, C9 and $(FAPbI_3)_x(MAPbBr_3)_{1-x}$ based perovskite in the (a) secondary-electron cut-off and (b) valence-band regions.

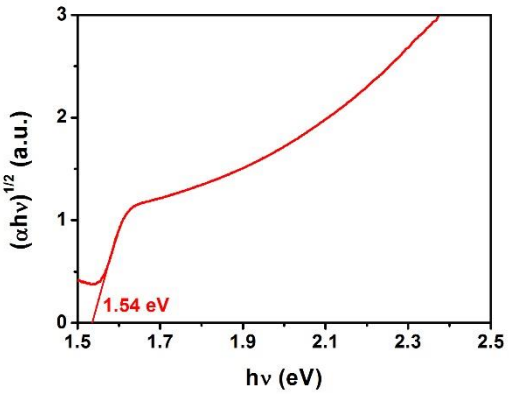

Fig. S9 The relationship of $(\alpha h\upsilon)^{1/2}$ vs energy for the perovskite film. The bandgap can be determined *via* linear extrapolation of the leading edges of the $(\alpha h\upsilon)^{1/2}$ curve to the base line.

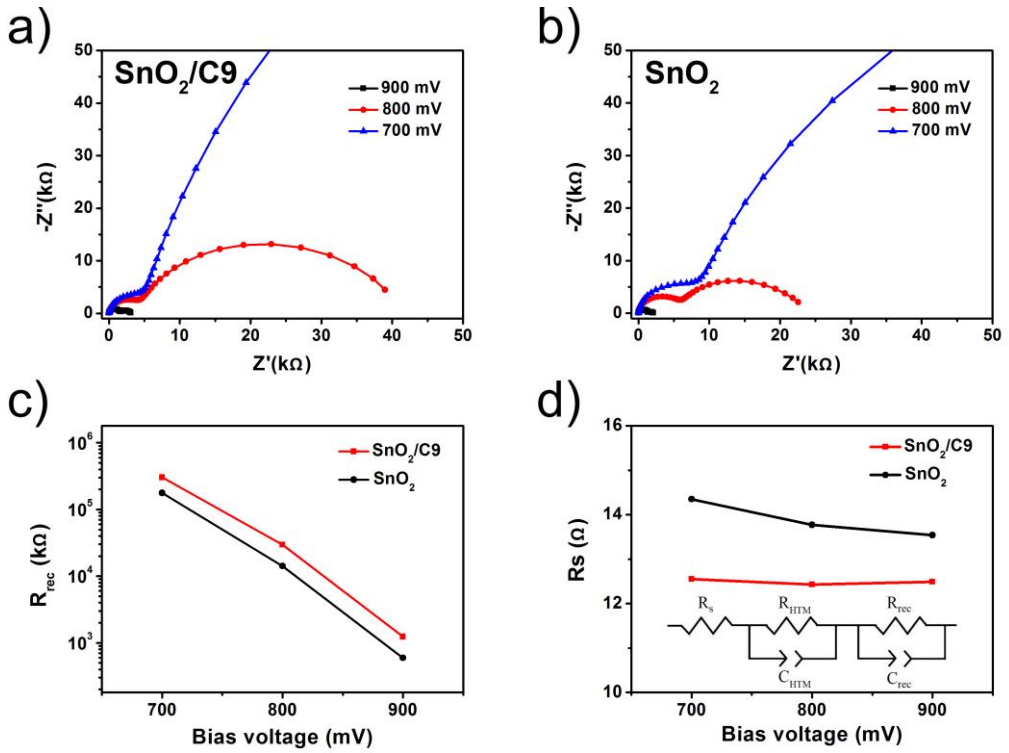

Fig. S10 Nyquist plots of representative devices based on (a) C9 modified SnO_2 and (b) bare SnO_2 ETL in the dark under 700, 800, 900 mV bias voltage. The relationship between bias voltages and (c) R_{rec} and (d) R_s for both devices. Inset: equivalent circuit for the simulation of charge transfer and recombination process.

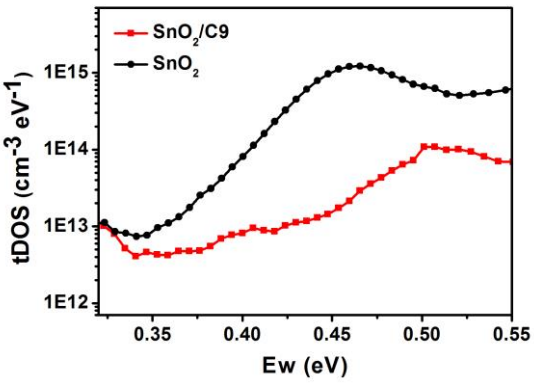

Fig. S11 TAS results for the perovskite films deposited on C9 modified and bare SnO_2.

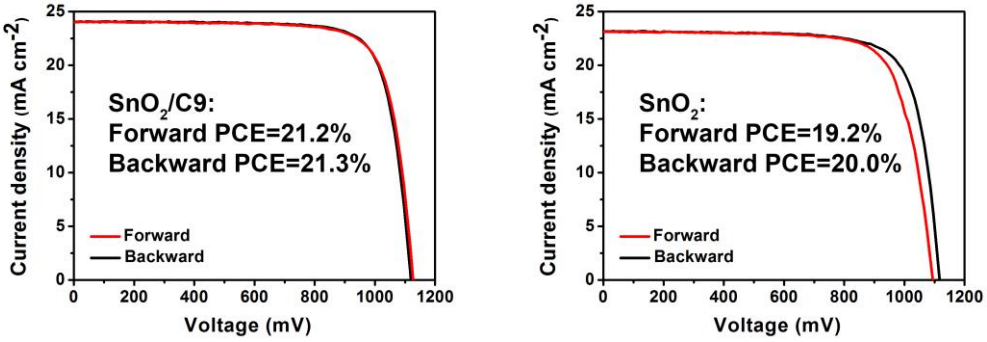

Fig. S12 Hysteresis effect in *J-V* curves for the best-performing PHJ PSCs based on C9 modified and bare SnO_2 ETL under different scanning directions.

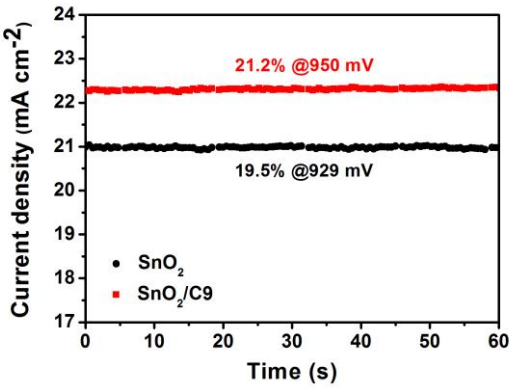

Fig. S13 The steady-state photocurrent output and stabilized PCE of the modified device based on SnO_2/C9 and the control device based on bare SnO_2 under their maximum power point.

Table S1. The band structure parameters of SnO_2, C9 and $(FAPbI_3)_x(MAPbBr_3)_{1-x}$ based perovskite.

Materials	Work function (eV)	Valance band maximum (eV)	E_g (eV)	HOMO (eV)	LUMO (eV)
SnO_2	4.17	3.68	3.71	7.85	4.14
C9	4.07	1.98	2.02	6.05	4.03
Perovskite	4.12	1.46	1.54	5.58	4.04

Table S2. Fitting parameters of bi-exponential decay function in time-resolved PL spectra.

Films	A_1	τ_1 (ns)	A_2	τ_2 (ns)	Average decay time τ (ns)[a]
Al_2O_3/perovskite	0.54	644.68	0.41	2032.48	1238.90
SnO_2/perovskite	0.30	82.82	0.67	248.47	197.26
SnO_2/C9/perovskite	0.30	62.68	0.67	160.61	130.17

[a] Average decay time is calculated according to the equation: $\tau = (A_1\tau_1 + A_2\tau_2)/(A_1 + A_2)$.

Table S3. Fitting parameters of bi-exponential decay function in TPV measurement.

Devices	A_1	τ_1 (ms)	A_2	τ_2 (ms)	Average decay time τ_v (ms)[a]
SnO_2/C9	0.79	0.09	0.18	8.47	1.65
SnO_2	0.81	0.07	0.17	2.42	0.48

[a] Average decay time is calculated according to the equation: $\tau_v = (A_1\tau_1 + A_2\tau_2)/(A_1 + A_2)$.

Table S4. Fitting parameters of bi-exponential decay function in TPC measurement.

Devices	A_1	τ_1 (μs)	A_2	τ_2 (μs)	Average decay time τ_c (μs)[a]
SnO_2/C9	0.60	1.03	0.60	1.03	1.03
SnO_2	0.41	1.21	0.41	1.21	1.21

[a] Average decay time is calculated according to the equation: $\tau_c = (A_1\tau_1 + A_2\tau_2)/(A_1 + A_2)$.

Table S5. Photovoltaic parameters of PHJ PSCs with different thickness of C9 modifying layer.

Devices	Concentration (mg mL^{-1})	J_{SC} (mA cm^{-2})	Calculated J_{SC} (mA cm^{-2})	V_{OC} (V)	FF (%)	H-index[a] (%)	PCE (%)
SnO_2/C9	5	23.1	21.9	1.10	76.1	0.9	19.3
	2	23.2	22.0	1.11	77.6	0.9	20.0
	1	23.5	22.2	1.11	78.1	0.8	20.4
	0.5	24.1	22.8	1.12	78.9	0.5	21.3
	0.2	23.8	22.5	1.12	77.9	1.7	20.6
SnO_2/PC_{61}BM	0.5	23.0	22.0	1.10	77.0	2.8	19.9

[a] H-index = $(PCE_{backward}-PCE_{forward})/PCE_{backward}$。